Four Independent Wheels Steering System Analysis

Article *in* SAE Technical Papers · April 2011

DOI: 10.4271/2011-01-0241

3 authors, including:

Paola Artuso
Università Telematica Guglielmo Marconi
12 PUBLICATIONS **77** CITATIONS
SEE PROFILE

Enrico Bocci
Università Telematica Guglielmo Marconi
61 PUBLICATIONS **673** CITATIONS
SEE PROFILE

11IDM-0056

Four independent wheels steering system analysis

ABSTRACT

In this paper a four independent wheel-steering system and its application on the HOST prototype are presented. The prototype is a heavy duty vehicle with four wheel motors controlled by wire, so that each wheel is mechanically not-linked to the other ones and has four degrees-of-freedom. Each wheel has an electric steering actuator to move the wheels around the steering axis, which is controlled by wire. The first part of the work deals with the model determination, reducing the four degree-of-freedom system into a one degree-of-freedom system. In the second part, the relationship between the rotations of each wheel and the linear movement of the electric steering is presented. In the third part the steering ratio is calculated and a parameter to reduce the slip angle is defined. In this way a four independent wheel steering model has been developed and applied to the specific characteristics of HOST. Finally the vehicle handling has been tested through simulations of steering-pad and moose-test, in order to verify the stationary and dynamic handling behavior. Despite the model is simplified, owing to the use of the corrective parameter, good performances in terms of turning radius, slip-angle and roll-angle are achieved, increasing maneuverability and stability.

INTRODUCTION

Since 1980's the development of four-wheel-steering vehicles has started and some cars have been commercialized [1]. A four-wheel-steering vehicle has the advantage to improve the vehicle cornering ability by steering the rear wheels in accordance to vehicle status. Using an appropriate steering control on the rear wheels, it is possible to improve also the lateral stability and in general handling performances [2-8] of the vehicle. At the beginning mechanical connections were used to make the integral steering [8], subsequently only the front axle was connected to the steering-wheel while the rear one was moved by another mechanism electronically controlled. A further evolution has been analyzed in the framework of the HOST project (2005/2009), which built up a prototype developed under the sixth European Framework Programme, coordinated by CIRPS-Sapienza, University of Rome [9]. The project objectives have been to develop a platform to host different cabs: car-sharing, collective taxi, garbage collection, freight distribution. In order to avoid any mechanical connections between the platform and the cabs, the prototype is a drive and steer-by-wire second generation hybrid vehicle [8] with four motor wheels, which are electronically controlled. To enhance the steering comfort and the vehicle safety, a steering model has been developed.

In literature, e.g. [2-7], models with two or three degrees-of-freedom are used to relate the wheel rotation about its steering axis to dynamic parameters as lateral or rolling speed of the vehicle or side-slip angles. In this work the reduction of the degree-of-freedom system to one has been considered using expressions which relate three wheels rotations to the one of the four wheels. In addition, in dynamic conditions, a parameter depending on vehicle speed [10] has been used to switch the out-of-phase to in-phase behavior [11]. Finally, another parameter has been introduced to reduce the slip-angle .

KINEMATICS ANALYSIS

The model used to simulate to steering conditions has been developed coming along several steps. In the first phase, the steering model has been the simplified two-wheels (bicycle) model; as reported in Figure 1, neglecting the slip-angle. Wheel rotation angles δ_f and δ_r are the degrees of freedom.

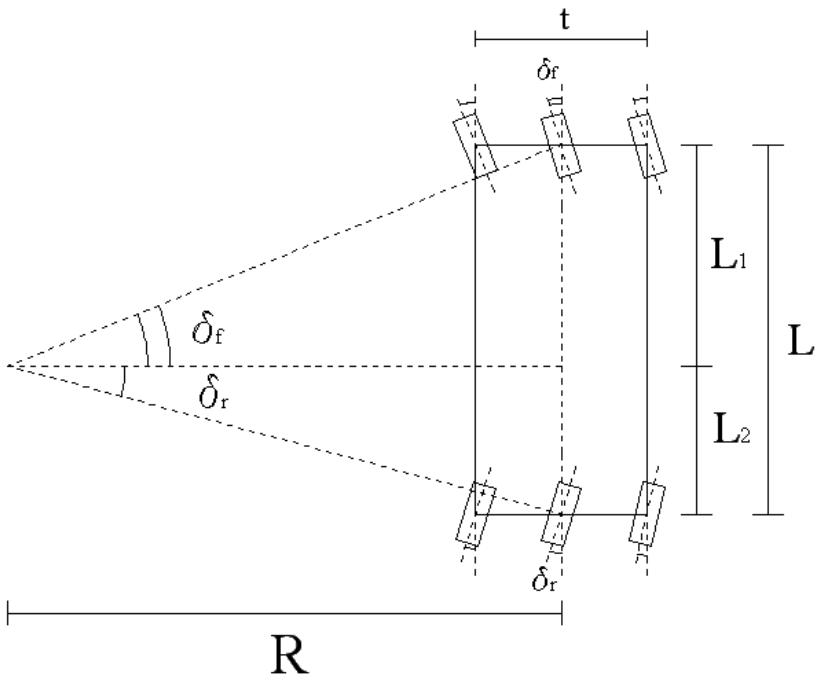

Figure 1: Bicycle model for cinematic steering [8].

Similar to [2, 3, 5], the parameter K is function of velocity as reported in eq. 1.

$$\delta_r = K(V) \cdot \delta_f \tag{1}$$

The simple bicycle model has two degrees-of-freedom, but the four-wheels model has four degrees-of-freedom .

The second step is to reduce to one the four wheels-rotations referring three of them to the front left wheel rotation δ^f_l. The following relations (2) and (3) express that δ_f and δ_r are the average rotations on the front and rear axles:

$$\delta_f = \frac{\delta_l^f + \delta_r^f}{2} \tag{2}$$

$$\delta_r = \frac{\delta_l^r + \delta_r^r}{2} \tag{3}$$

where δ^f_r is the front right wheel rotation, δ^r_l the rear left wheel rotation, δ^r_r the rear right wheel rotation. It is possible to express the wheel-base L as sum of two distances L_1 and L_2 shown in figure 1:

$$L = L_1 + L_2 \tag{4}$$

To complete the system, other four equations are introduced:

$$\tan \delta_l^f = \frac{L_1}{R - \frac{t}{2}} \tag{5}$$

$$\tan \delta_r^f = \frac{L_1}{R + \frac{t}{2}} \tag{6}$$

$$\tan \delta_l^r = \frac{L_2}{R - \frac{t}{2}} \tag{7}$$

$$\tan \delta_r^r = \frac{L_2}{R+\frac{t}{2}} \quad (8).$$

Where *t* is the track of vehicle, R is the distance of the instantaneous centre of rotation to its projection on the centre line of the vehicle (figure 1). As (5), (6), (7), and (8) are trigonometric equations, in order to simplify the calculus, at low rotation angles, it is possible to assume:

$$\tan \delta \cong \delta \quad (9)$$

The error (in terms of degree) occurred using (9) is reported in Figure 2. On the horizontal axis there is the rotation angle of the wheel, while the vertical axis shows the error.

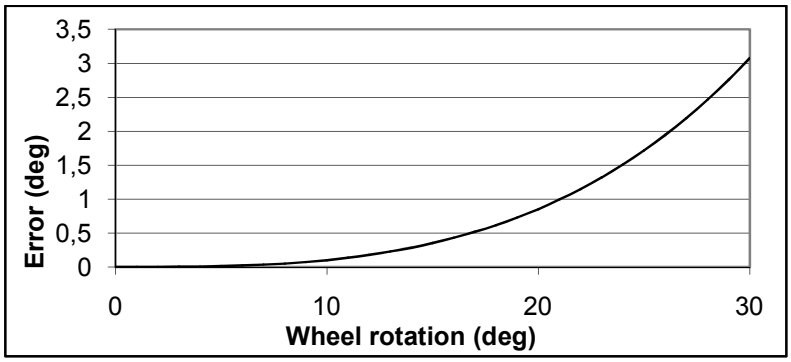

Figure 2: Error related to the approximation of the equation (9).

Considering 30° is the maximum steering angle, (9) introduces an acceptable 10.1% error equivalent to 3.1°. In this way the equations (5), (6), (7) and (8) respectively become the equations (10), (11), (12) and (13):

$$\delta_l^f \cong \frac{L_1}{R-\frac{t}{2}} \quad (10)$$

$$\delta_r^f \cong \frac{L_1}{R+\frac{t}{2}} \quad (11)$$

$$\delta_l^r \cong \frac{L_2}{R-\frac{t}{2}} \quad (12)$$

$$\delta_r^r \cong \frac{L_2}{R+\frac{t}{2}} \quad (13)$$

The solution of the system formed by eq. (1), (2), (3), (4), (10), (11), (12) and (13) is reported as equations (14), (15) and (16):

$$\delta_r^f = \frac{2-\frac{t}{L}(1+K)\delta_l^f}{2+\frac{t}{L}(1+K)\delta_l^f}\delta_l^f \quad (14)$$

$$\delta_l^r = K \cdot \delta_l^f \quad (15)$$

$$\delta_r^r = K\frac{2-\frac{t}{L}(1+K)\delta_l^f}{2+\frac{t}{L}(1+K)\delta_l^f}\delta_l^f \quad (16)$$

STEERING MODEL DEFINITION

In order to reduce the slip-angle, the parameter S has been introduced and it represents an increase to external turning wheels. S is function of δ^f_l: in the corner with short radius it is higher than in the other with long radius. In the left turning corners the new rotations are defined as in (17), (18), (19) and (20):

$$\overline{\delta_l^f} = \delta_l^f \tag{17}$$

$$\overline{\delta_r^f} = S\left(\delta_l^f\right) \cdot \delta_r^f \tag{18}$$

$$\overline{\delta_l^r} = \delta_l^r \tag{19}$$

$$\overline{\delta_r^r} = S\left(\delta_l^f\right) \cdot \delta_r^r \tag{20}$$

In the right corner the new rotations are defined as in (21), (22), (23) and (24):

$$\overline{\delta_l^f} = S\left(\delta_l^f\right) \cdot \delta_l^f \tag{21}$$

$$\overline{\delta_r^f} = \delta_r^f \tag{22}$$

$$\overline{\delta_l^r} = S\left(\delta_l^f\right) \cdot \delta_l^r \tag{23}$$

$$\overline{\delta_r^r} = \delta_r^r \tag{24}$$

Each wheel is controlled by an electric motor; in this way the steering rotation has to be related to the displacement of the corresponding electric actuator Δ_l^f. By the geometry of the steering-system, showed in Figure 3, $\overline{\delta_l^f}$ is related to Δ^f_l (displacement of the electric actuator) by the equation (25):

$$\overline{\delta_l^f} = \frac{\varepsilon \cdot \pi}{180} - arcos\left(\frac{b^2+c^2-d^2-\Delta_l^{f\,2}+\Delta_l^f\sqrt{d^2+e^2}}{2b \cdot c}\right) \tag{25}$$

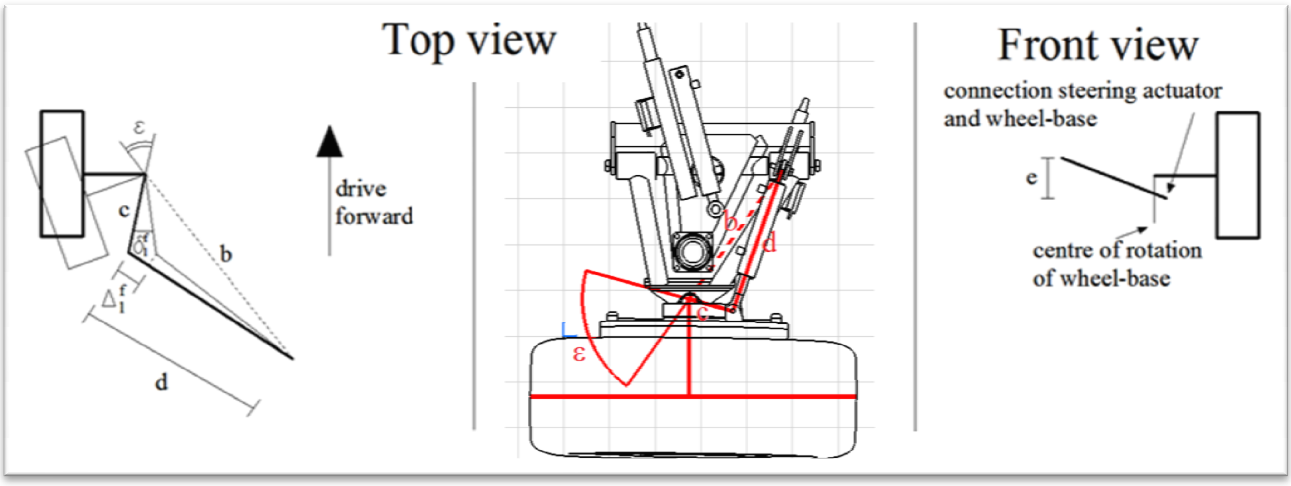

Figure 3: Geometric schematization of the front left steering actuator. This representation can be applied to the other wheel, except for their side and the drive sense.

While Δ^f_l is the input for the system, Δ^f_r,Δ^r_l,Δ^r_r are the outputs and they depend on the corresponding wheel-rotations as reported in the equations (26), (27), (28):

$$\Delta_r^f = \sqrt{b^2 + c^2 - 2b \cdot c \cos\left(\frac{\varepsilon \cdot \pi}{180} + \overline{\delta_r^f}\right) + e^2} - \sqrt{d^2 + e^2} \tag{26}$$

$$\Delta_l^r = \sqrt{b^2 + c^2 - 2b \cdot c \cos\left(\frac{\varepsilon \cdot \pi}{180} + \overline{\delta_l^r}\right) + e^2} - \sqrt{d^2 + e^2} \tag{27}$$

$$\Delta_r^r = \sqrt{b^2 + c^2 - 2b \cdot c \cos\left(\frac{\varepsilon \cdot \pi}{180} + \overline{\delta_r^r}\right) + e^2} - \sqrt{d^2 + e^2} \quad (28)$$

The Figure 4 shows the flow-sheet of the steering model.

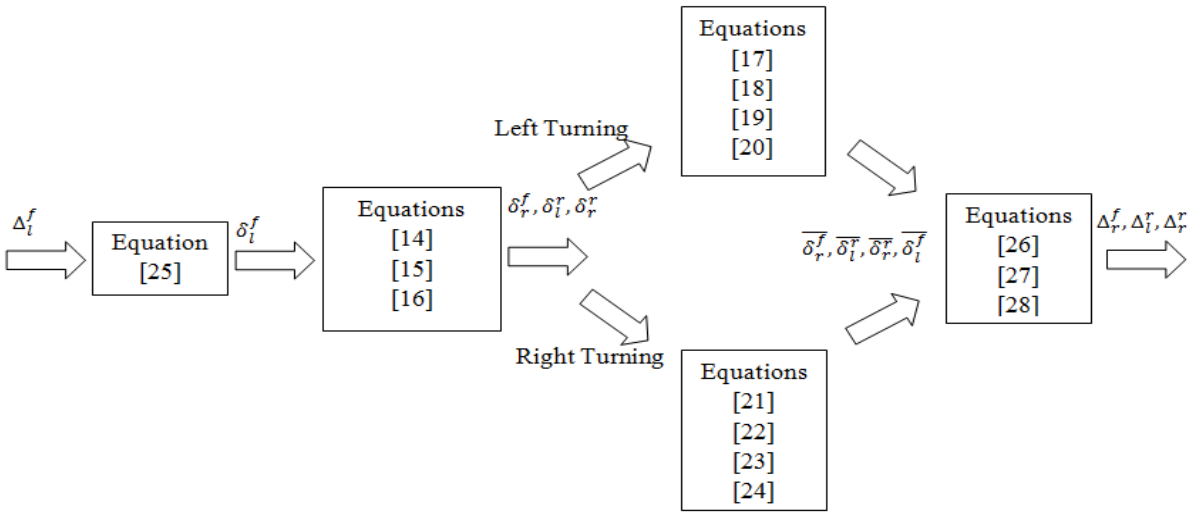

Figure 4: Flow-sheet of the steering model.

PARAMETERS COMPUTATION

To proceed to the dynamic analysis of the steering system, both the parameter K of the equation (15) and S of the equation (18 and 20) or (21 and 23) have to be defined as functions of velocity and steering rotation respectively. The definition of K and S values is based on virtual simulation test realized by means of the software *SIMPACK*. This is a multibody simulation software which allows dynamics analysis of any mechanical or mechatronic system, thus calculating the motion of multi-body systems as well as forces and accelerations and vibrational behavior [12]. The basic concept of *SIMPACK* is to create the equations of motion for mechanical and mechatronic systems and then from these equations, apply various different mathematical procedures to produce a solution (e.g. time integration). The *SIMPACK* model is built up using the *SIMPACK* modeling elements and defining the internal and external forces. *SIMPACK* will then automatically generate the system equations from this model.

The intent was to maintain an under-steering behavior and reduce slip-angle. The hypothesis has been to concentrate the sprung mass in only two body (front and rear), use the default contact between tires and road data of SIMPACK, considering the air resistance (drag force) only on the forward direction. The Figure 5 shows the HOST *SIMPACK* model and the HOST prototype. The data input of the program is the geometry and weight of the vehicle which are:

- suspension weight: 177.89 kg;
- chassis front mass: 815.46 kg;
- chassis rear mass: 922.31 kg;
- wheel base L: 3000 mm;
- track t: 1725 mm.

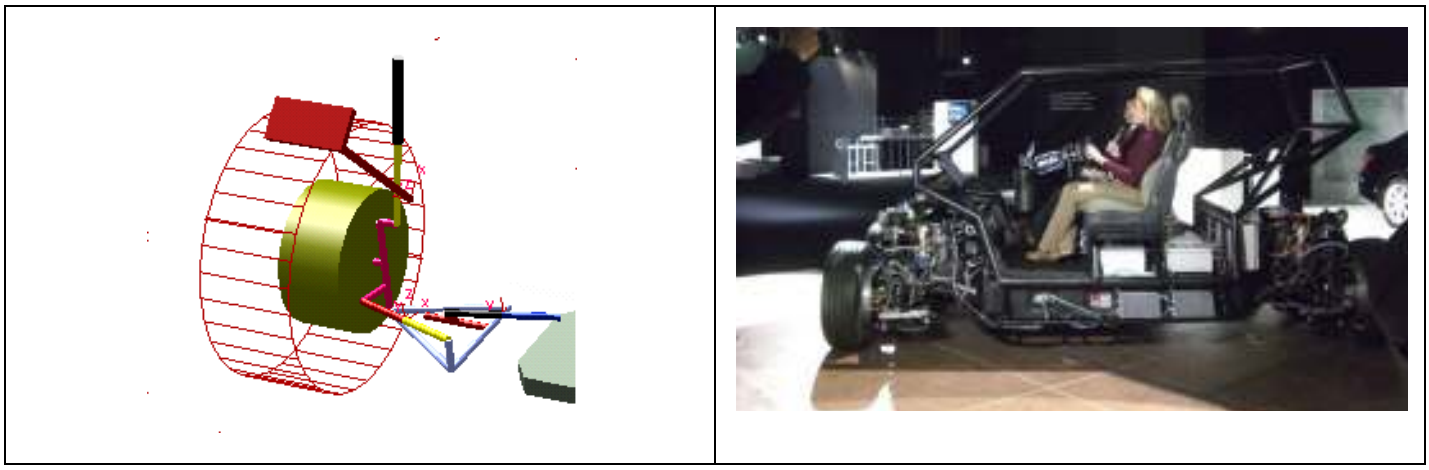

Figure 5: HOST SIMPACK model and HOST prototype.

In addition, the other input is the steering wheel angle and the velocity. The outputs of the program are K and S. The global inputs-outputs are showed in the Figure 6.

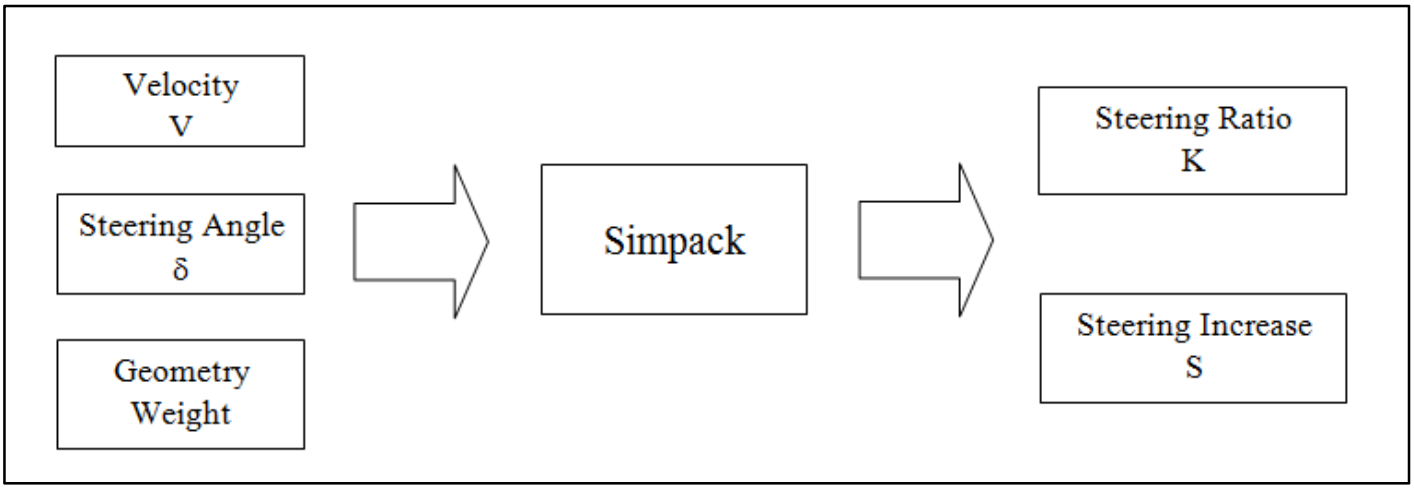

Figure 6. Input-output Simpack

As K is function of velocity, its value has to be determined by an interpolation curve. On that curve there are three very important points: K=0, maximum K, minimum K. K = 0 corresponds to the transient value from out-of-phase to in-phase wheels rotation. By a series of steering-pad simulations with K = 0 and speeds from 0 to 80 km/h, the transient value has been set to 50 km/h. Figure 4 reports the trend of maximum front and rear tire slip angle versus speed.

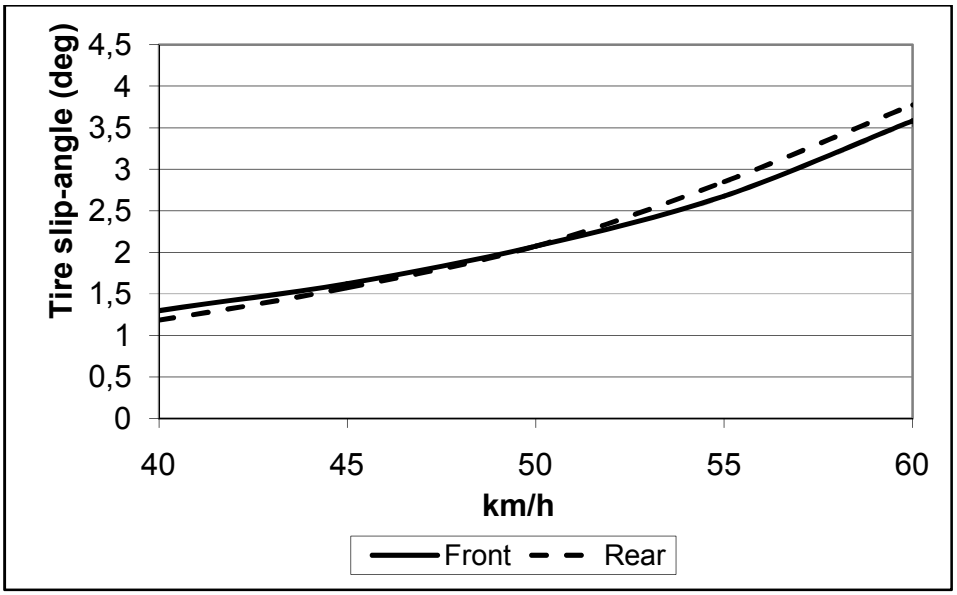

Figure 7: Front and rear tire slip-angle versus vehicle speed with K=0%.

Considering the tire forces saturated, while front slip angle is higher than rear, the vehicle has an under-steering behavior which is the target to be maintained under all driving conditions; when speed is over 50 km/h there is over-steering behavior, then it is necessary to turn the rear wheels in phase with the front ones and this corresponds to K > 0.

To determine the maximum K value, tests have been carried out at high speed (up to 120 km/h) with 0.56 g maximum acceleration. In the figure 8 four lines represent the slip angle versus lateral acceleration g in four cases (K = 10%; 20%; 30%; 40%) in the worst conditions, which are related to the anterior right wheel. As for K higher than 30% there is not a significant reduction of slip angle, K = 30% at 120 km/h is the final choice.

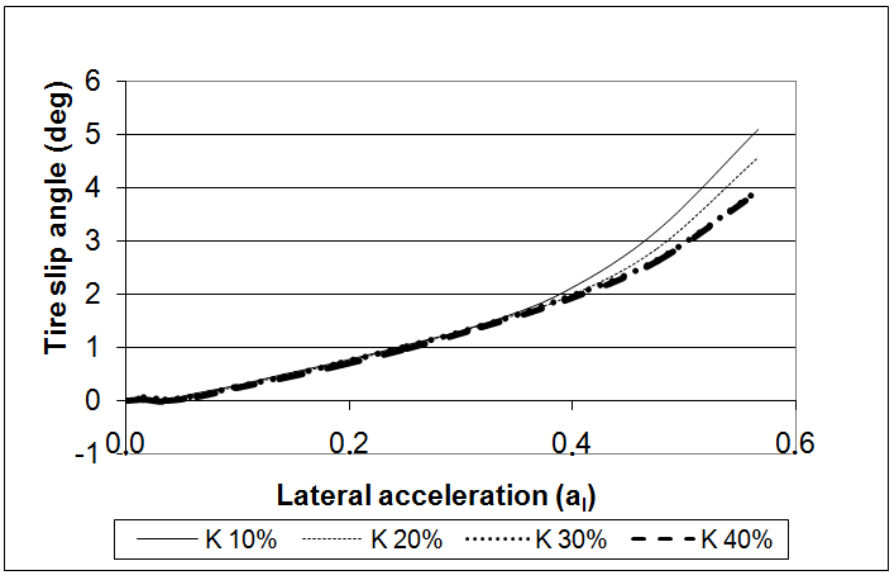

Figure 8: Maximum tire slip angles for four different K values.

The minimum K is negative because the rear wheels rotation is out-phase in comparison to front rotation. Figure 9 represents five cases (K = 0%; -10%; -20%; -50%; -70%) in the worst conditions, which are related to the anterior right wheel, for tire slip angle plotted versus lateral acceleration a_l obtained in steering-pad tests with 20 m cornering radius and 40 km/h maximum speed

(equivalent to 0.63 g lateral acceleration); until $a_l < 0.36$ g, increasing K the maximum slip angle of front tires decreases down to K = -70%. When $a_l > 0.36$ g the lower is K, the lower is the slip angle, even thought for K = 0 – 10 – 20% the effect is not so evident.

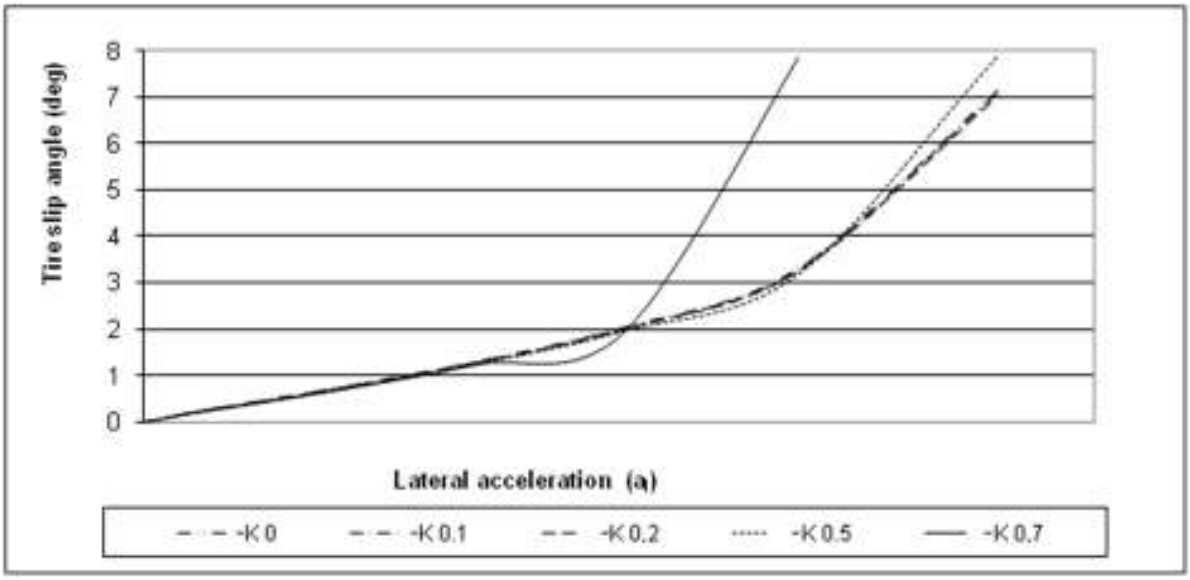

Figure 9: Maximum tire slip angle for five different K values at 40 km/h in a corner with 20 m as radius.

At -80 % vehicle has an over-steering behavior because rear tire slip angle is greater than front tires at every lateral acceleration, as reported in Figure 10. For these reasons, the minimum value is K = -70% at minimum velocity (close to 0 km/h).

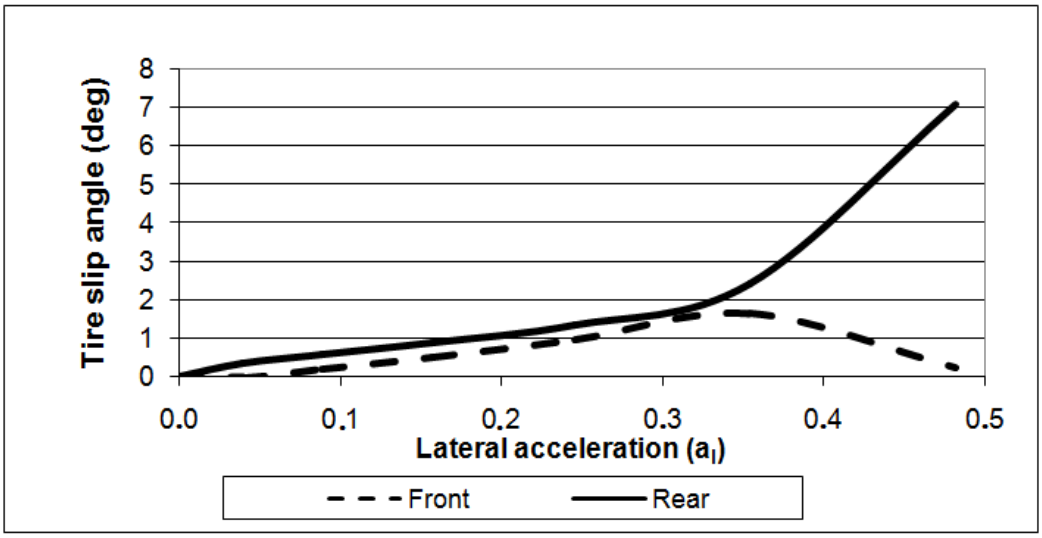

Figure 10: Front and rear tire slip angle versus lateral acceleration at K = -80%.

Stated these three values, the other ones are set by simulating the steering-pad tests at different K values to minimize tire slip angles for different speeds. Figure 11 shows the curve of factor K. This line is composed by two cube curves fitting K values at which tire slip angles decrease. The two corresponding equations are (25), (26):

$$K_I = \sqrt[3]{0.024696 \cdot V - 0.343} \tag{25}$$

$$K_{II} = \sqrt[3]{\frac{0.0972}{70} \cdot V - 0.027 \cdot \frac{5}{7}} \tag{26}$$

where V is the vehicle speed, K_I is referred to the first step up to 50 km/h, K_{II} stands for the second step up to 120 km/h (HOST maximum speed).

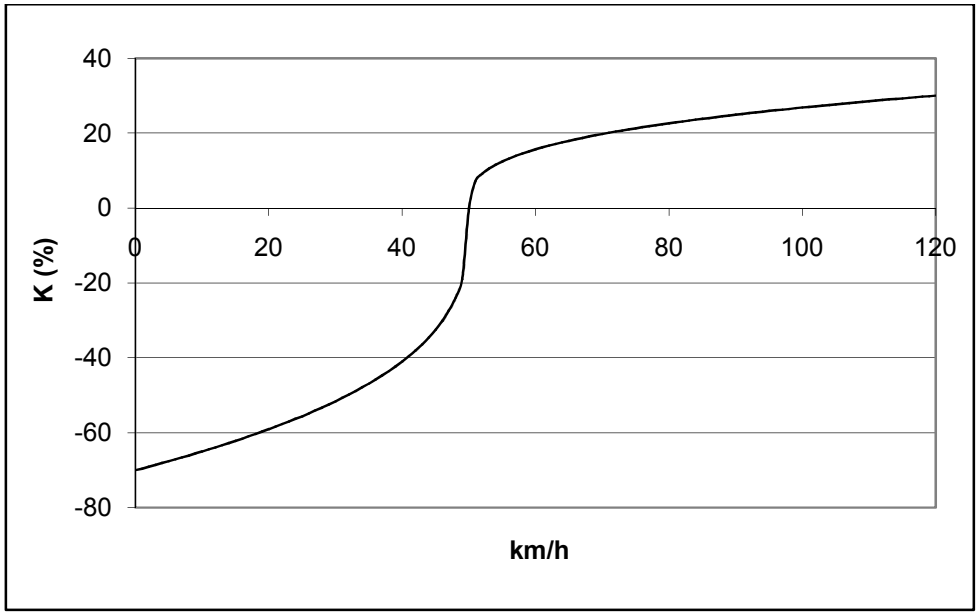

Figure 11: K profile versus vehicle speed.

In order to decrease maximum slip angle, during the cornering, the rotation of external turning wheels has been increased of a factor S depending on rotation of front left wheel (assumed as reference). By steering-pad has been determined the best S value at each velocity. As there are two cases, turn left and turn right, there are two S equations. Figure 12 shows the best fitting curve for left corner and its equation is (27):

$$S^{+} = \sqrt{0.124 \cdot \delta_l^f} + 1 \tag{27}$$

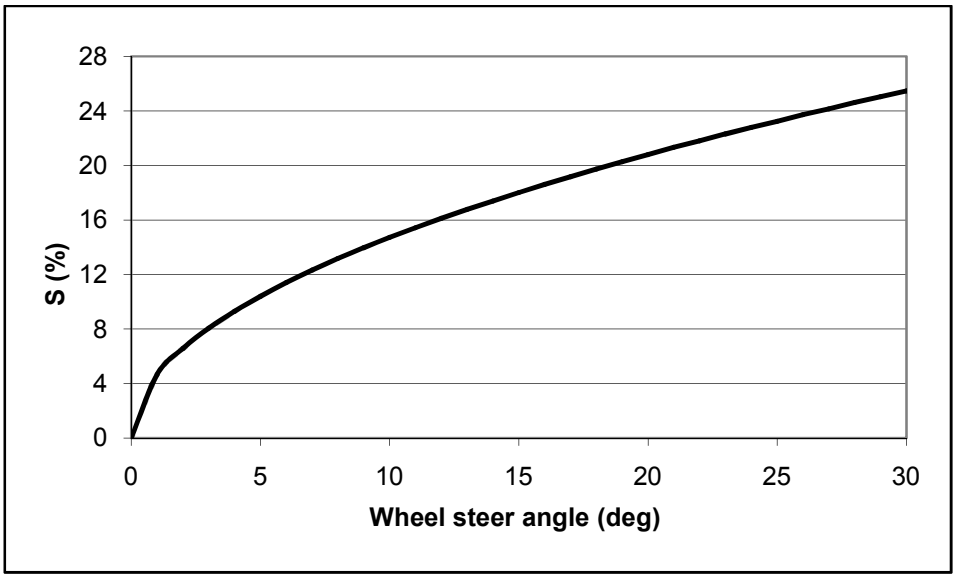

Figure 12: S profile versus front left wheel steer angle in left cornering.

Figure 13 presents the curve for right corner and its equation is (28):

$$S^{-} = \sqrt{-0.128 \cdot \delta_l^f} + 1 \tag{28}$$

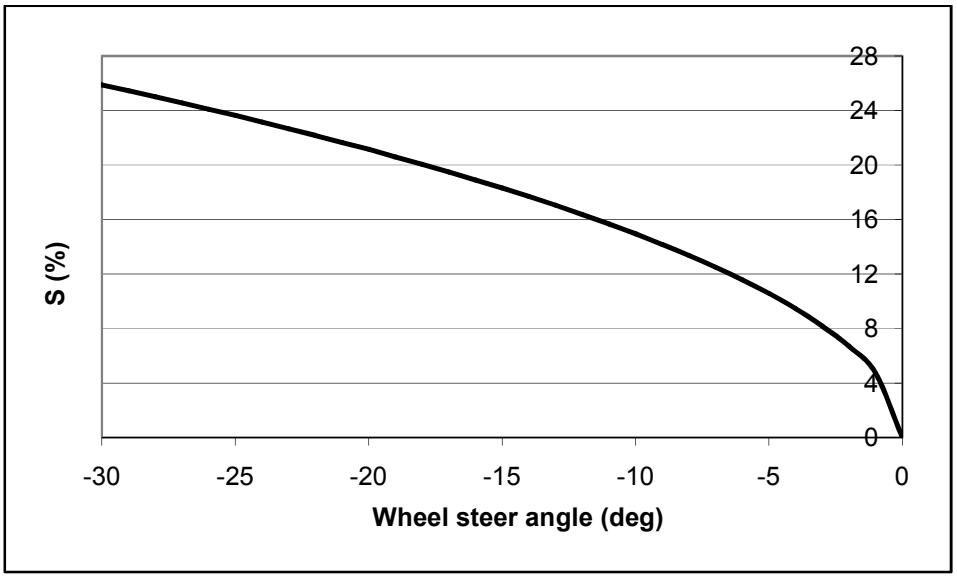

Figure 13: S profile versus front left wheel steer angle in right cornering.

The maximum steering increase is 25.5%. This is the value correspondent to lower maximum value of tire slip angle. In Figure 14, it is possible to see that, for S over 25.5%, there is not a significant decrease of maximum slip angle.

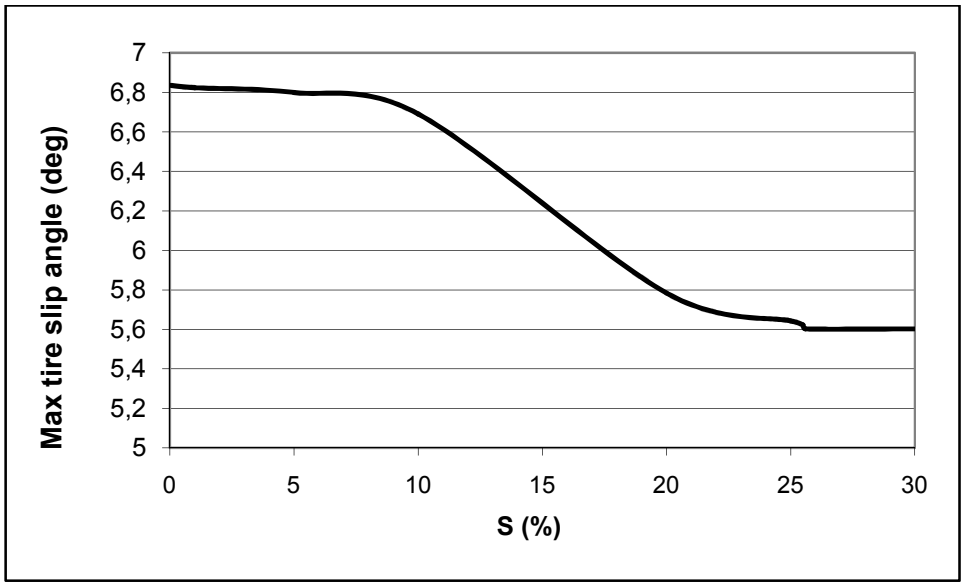

Figure 14: Maximum tire slip angle versus S values.

DYNAMIC SIMULATIONS RESULTS

The final part of this paper is dedicated to simulations which show the effects of the steering model. To evaluate the vehicle's behavior under stationary and dynamic conditions, two simulated tests have been used:

- steering-pad test;
- moose test.

The curve in Figure 15 is the final HOST's behavior with the steering algorithm developed in this work during the steering-pad tests. Maximum slip angle corresponds to 5.5° at 0.63 g as lateral acceleration.

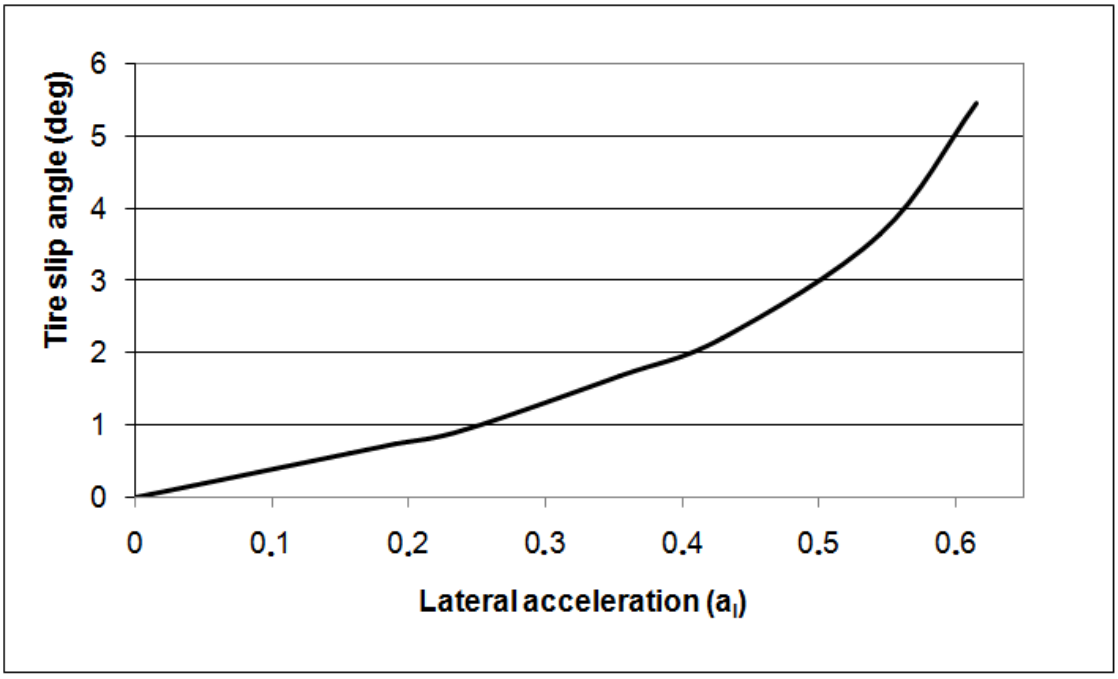

Figure 15: Tire slip angle in steering-pad tests.

About roll-angle, the final result is presented in Figure 16. This graph presents the values on center of gravity versus lateral acceleration of vehicle. The maximum value is 4.5°, besides a quasi-linear behavior is observed and it is acceptable because the roll velocity is quasi-constant.

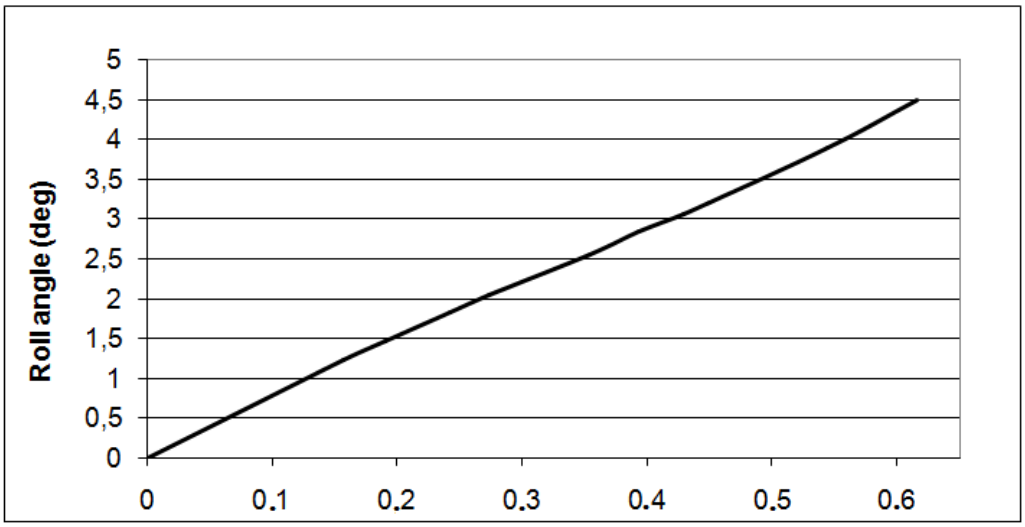

Figure 16: Roll angle in steering-pad tests.

Thanks to four-wheels-steering system, HOST could drive trajectory down to 3.7 m radius; this result comes from a steering pad at 10 km/h. Experimental tests on commercial 4WS vehicles showed at same speed same radius but with lower weight, wheel base and track than HOST (e.g. Renault Laguna 4WS model: weight 1,638 kg, wheel base 2.756 m, front track 1.557, rear track 1.512).

The second trial for the evaluation is the “moose test”. The target was to establish maximum velocity at which the vehicle completes the test. Moose test was repeated with an increasing speed until the vehicle either skids down the cones or spins around. The maximum velocity reached is 40 km/h. In Figure 17 the curves for front and rear slip angles during the test at 40 km/h are reported.

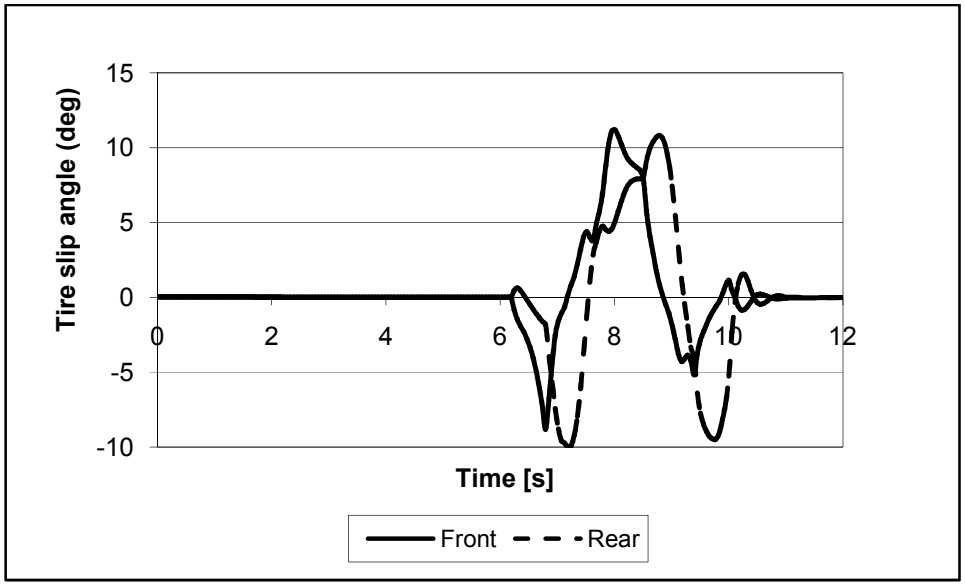

Figure 17: Front and rear tire slip angles during moose-test at 40 km/h.

Up to 6.2 seconds there is not slip angles due to straight track, then there is a left curve which origins negative values, after that a right curve with positive angles and finally the vehicle goes along another straight track. The graph in Figure 17 shows a similar behavior for the wheels on the same axis, especially on the rear. There is a delay time of 0.3 seconds from front and rear angles due to the steering mode. This entails an over-steering behavior during the three changes of direction, although HOST completed the test.

With regards to steering pad the maximum value registered for slip angles is 5°. During the moose test, the maximum value for slip angle is 11.2° which is much higher than the other one and the results of [5, 6]. Anyway we should take into account that the moose is a dynamic test characterized by sudden changes of direction, so that a higher value is acceptable.

Even roll-angle is higher than steering-pad, but this time the difference is only about one degree. In Figure 18 the roll-angle is reported The maximum value is 5.2° (as absolute value) which is near to 4.5° registered in steering pad.

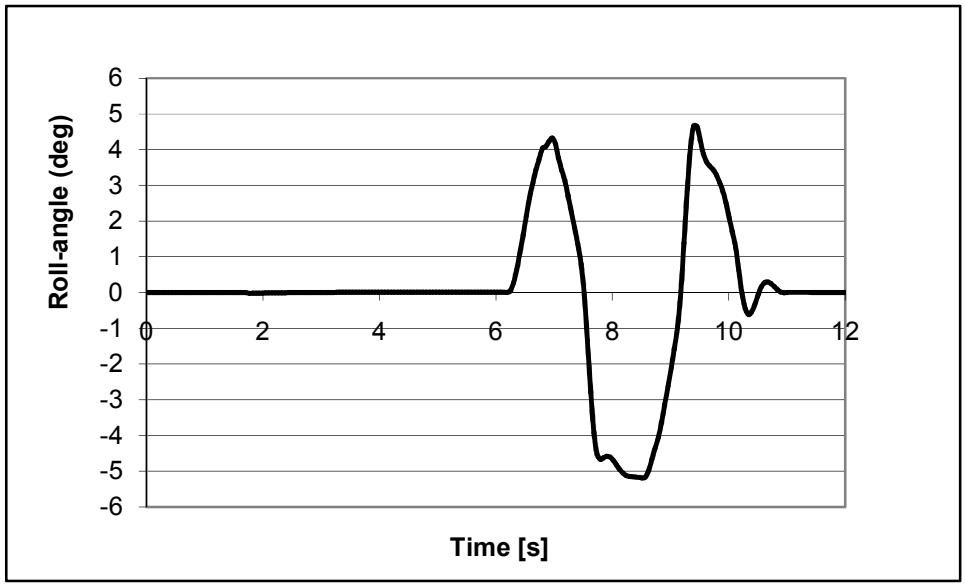

Figure 18: Roll angle during moose-test at 40 km/h.

CONCLUSIONS

In this paper, a new steering model for a four-wheels-steering vehicle has been presented. The four wheels are independent each other, but the developed model proposes the relationships between the reference wheel and the other three wheels. In this way the four degree-of-freedom system is reduced to a one degree-of-freedom system, simplifying the model in comparison with two or three degrees-of-freedom systems described in literature. The model, designed for an existing prototype, is based on speed and wheels steering angles. The vehicle handling has been tested through SIMPACK simulations of steering-pad to find out only two parameters (K and S) that will define the wheels steering angles and reduce the slip-angle. K indicates the rear steering based on the front steering angle. S indicates the increase of the steering value at the external wheels in order to reduce the slip-angles. Thus a simplification of the model can be accepted if a corrective parameter is implemented. Indeed final results showed good performances in turning radius, slip-angle and roll-angle, increasing maneuverability and stability.

1. References

[1] Giancarlo Genta, Meccanica dell'autoveicolo, Levrotto&Bella 1993, p.303

[2] Spentzas KN, Alkhazali I, Demic M, Kinematics of four-wheel-steering vehicles, ForschungimIngenieurwesen 66 (2001), pp. 211-216

[3] Spentzas KN, Alkhazali I, Demic M, Dynamics of four-wheel-steering vehicles, ForschungimIngenieurwesen 66 (2001), pp. 260-266

[4] Chen Ning, Chen Nan, Chen YanDong, On fractional control method for four-wheel-steering vehicle, Science in China Series E: Technological Science (2009), pp. 603-609

[5] Fan Lu, Modeling and Simulation of Four Degree-of-Freedom Four-Wheel-Steering Vehicle, Proceedings of 2010 WASE International Conference on Information Engineering, Beijing, China

[6] Hwan - Seong - Kim and Sam - Sang You, Estimation of Vehicle Sideslip Angle for Four - Wheel Steering Passenger Cars, Transactions on Control, Automation and System Engineering Vol. 3 No 2, June 2001

[7] Li Zhou, Linli Ou & Cui Wang, A Simulation of the Four-Wheel Steering Vehicle Stability Based On DYC Control, Proceedings of 2009 International Conference on Measuring Technology and Mechatronics Automation, pp. 189 – 193, Zhangjiajie, Hunan.

[8] Shibahata Y, Progress and future direction of Chassis control technology, Annual Reviews in Control 29 (2005), pp. 151-158

[9] www.hostvehicle.eu

[10] Sano S, Furukawa Y, Shiraichi S, Four-wheel-steering system with rear wheel steer angle controlled as a function of steering wheel angle, SAE Paper (1986) No. 860625, pp. 363-365

[11] Thomas D. Gillespie, Fundamentals of vehicle dynamics, SAE International, pp. 201, 302

[12] http://www.simpack.com/

[13] Horiuchi S, Okada K, Nohtomi S, Improvement of vehicle handling by nonlinear integrated control of four wheel steering and four wheel torque, JSAE Review 20 (1999), pp. 459-464

[14] Cho YH, Kim J, Design of four-wheel-steering system, Vehicle System Dynamics 24 (1995), pp. 661-682

CONTACT INFORMATION

ENG. RONCI ROBERTO RONCI.ROBERTO@GMAIL.COM

ENG. JOEL FERRER JOEL.FERRER@UNIROMA1.IT

PHD. PAOLA ARTUSO PAOLA.ARTUSO@UNIROMA1.IT

PHD. ENRICO BOCCI ENRICO.BOCCI@UNIROMA1.IT

ACKNOWLEDGMENTS

The research has been supported from 2003 to 2008 by European Commission in the framework of the 6FP; and from 2008 to 2010 from “Assessorato all’Ambiente e alla Cooperazione tra i popoli” of the Lazio Region, in the framework of the Programme “Polo IdrogenoLazio” (2006-2010)”.